Proceedings of the Fifteenth International Conference on
Computational Structures Technology
Edited by: P. Iványi, J. Kruis and B.H.V. Topping
Civil-Comp Conferences, Volume 9, Paper 3.1
Civil-Comp Press, Edinburgh, United Kingdom, 2024
ISSN: 2753-3239, doi: 10.4203/ccc.9.3.1

Text-Guided Bio-Architectured Materials Library Building and Application to Structural Design

Y. Wang[1], W. Zhang[1], X. Guo[1] and S.-K. Youn[2]

[1]Department of Engineering Mechanics, Dalian University of Technology, China
[2]Department of Mechanical Engineering, Korea Advanced Institute of Science and Technology
Daejeon, Republic of Korea

Abstract

Advancements in deep learning techniques have not only enhanced intuitive data analysis in structural design but have also facilitated the transfer of deep-level information. The microstructural features of biomaterials, termed "structural genes," inspire engineering design with their uniqueness and complexity, containing a wealth of potential optimization resources. Structural genes are categorized into three main groups based on their functions: structure and mechanical properties, fluid dynamics and substance exchange, and energy management and interaction. The construction of a deep information database founded on these structural genes adds a new dimension to materials science research and revitalizes structural optimization methods. This study refines the text-to-image model to construct a biomaterials database, integrating it into the topology optimization design. This integration allows the design process to incorporate nature's optimization strategies, generating engineering structures that meet mechanical requirements and possess bio-inspired characteristics. Experimental validation presented in this paper showcases a novel paradigm for functional biomimetic design.

Keywords: deep learning, topology optimization, structural genes, text inversion, bio-inspired design, materials library.

1 Introduction

Biomaterials in nature possess unique microstructural traits, revealing vast potential in engineering and materials science. Their microstructures grant remarkable mechanical and multiphysical properties. This has garnered substantial research

interest [1]. The application value lies in their capacity to inspire the development of new materials. These materials are lighter, stronger, and environmentally aligned. In-depth research and comprehension of these bio-microstructures could propel materials science. It could also direct future engineering design trends.

Microstructures can be categorized into three types based on function, as shown in Figure 1.

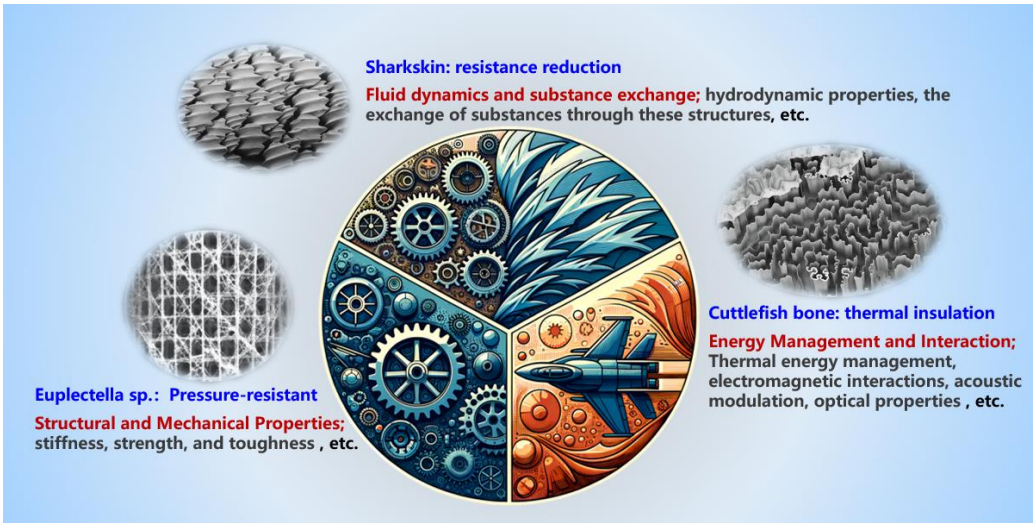

Figure 1: Diagram illustrating the three categories of structural genes.

Structure and mechanical properties; the physical and mechanical attributes of biological microstructures, such as stiffness, strength, and toughness, reflect the organism's mechanical adaptation to its structure. Examples include the Euplectella sp., nautilus, and ammonite sutures, etc. [2].

Fluid dynamics and substance exchange; the interaction between biological microstructures and fluids (liquids and gases), including fluid dynamic characteristics (such as lift and resistance), and the substance exchange (such as the transport of water and gases) conducted through these structures. Examples include dragonfly wings, shark skin, etc. [3-4].

Energy management and interaction; the interaction of biological microstructures with various forms of energy can be further subdivided into:

Thermal energy management and electromagnetic interaction: involve thermal effects such as absorption, emission n, and insulation of heat, as well as reflection, transmission, and absorption of electromagnetic waves, including biologically generated electrical signals. Examples include cuttlefish bone [5].

Acoustic regulation: relates to the generation, propagation, and absorption of sound waves, including how microstructures affect acoustic properties. An example is the sonar-camouflaging earless moth [6].

Optical properties: encompass reflection, refraction, scattering, and absorption of light, along with the visual effects produced by these processes. Examples include the Troides urvillianus and biophotonic gyroid materials T.opisena [7-8].

Structural topology optimization is an essential design method that aims to enhance performance for specific functions through material layout optimization. Its application has extended from purely mechanical structures to micro and macroscopic issues in heat exchange, piezoelectrics, fluids, and other physical fields. However, integrating topology optimization with biomimetic design, particularly in simulating complex biological microstructures, remains a significant challenge. Current research has made some progress but still falls short in accurately capturing the finesse, complexity, and functional relationships of biological microstructures. Moreover, current topology optimization methods often require substantial computational resources when addressing multi-scale and multifunctional structural design problems, limiting their application in engineering practice.

Meanwhile, the rapid advancement of machine learning offers new research methodologies for bionics and materials science. By learning from and extending the features of biological microstructures, machine learning can not only increase the efficiency of structural design but also reveal complex patterns inherent in biological materials. Although studies have successfully applied machine learning techniques to achieve breakthroughs in bionics, these achievements are often limited to specific applications and are difficult to generalize to complex material systems. Therefore, establishing a comprehensive database of biomaterials, integrating deep information about bio-microstructures while considering the interconnected needs of functional characteristics and engineering applications, is crucial for enhancing the efficiency and effectiveness of biomimetic design in materials science.

In this article, similar to how the arrangement of atoms within the material genome dictates material properties, 'structural genes' are defined as specific forms of material distribution that manifest unique structural performance. These abstract contents are translated from written descriptions into tangible image representations through text-to-image generation and are propagated as structural genes within topology optimization. Going further, a structural gene database can be constructed via the text-to-image model, facilitating the creation of innovative structures rich in experience and information. This approach aims to surmount the challenges of indistinct design requirements that cannot be met due to limitations in human experience or inadequate data.

2 Methods

The construction of a material library does not require training. The fine-tuning model used in this article is based on the Latent Diffusion Model (LDM) [9]. The LDM comprises two main components. The first component consists of an encoder and a decoder. The encoder, $\mathcal{E}$, is trained to learn the mapping of an image $x \in \mathcal{D}_x$ to a latent space encoding $z = \mathcal{E}_{(x)}$. The decoder, D, learns to map these latent encodings

back to the original image, satisfying $D(\mathcal{E}_{(x)}) \approx x$. The second component is a diffusion model trained to generate encodings within the learned latent space. Let $c_\theta(y)$ be the model that maps a conditional input y to a conditional vector. Thus, the loss function for the LDM is:

$$L_{LDM} \coloneqq \mathbb{E}_{z\sim\mathcal{E}_{(x)},y,\epsilon\sim\mathcal{N}(0,1),t}\left[\left\|\epsilon - \epsilon_\theta\left(z_t, t, c_\theta(y)\right)\right\|_2^2\right] \quad (1)$$

The variable t denotes the time step, z_t represents the latent noise at time t, ϵ is the unscaled noise sample, and ϵ_θ represents the denoising network. During training, c_θ and ϵ_θ are jointly optimized to minimize the loss of the LDM. In the inference phase, a random noise tensor is sampled and a new image's latent value z_0 is generated through an iterative denoising process. Finally, the latent code is transformed into an image by the pre-trained decoder $x' = D(z_0)$.

The article employs the text-to-image model made publicly available by Rombach et al. [9], which contains 1.4 billion parameters and has been pre-trained on the LAION-400M dataset [10]. Here, c_θ is implemented using the BERT text encoder [11], where y denotes the text prompt. In the research conducted by Gal et al. [12], the embedding space (also known as the latent space) is chosen as the target for inversion. The optimization objective can be defined as:

$$v_* = \arg\min_v \ \mathbb{E}_{z\sim\mathcal{E}_{(x)},y,\epsilon\sim\mathcal{N}(0,1),t}[\|\epsilon - \epsilon_\theta(z_t, t, c_\theta(y))\|_2^2] \quad (2)$$

The implementation is achieved by repetitively employing the same training scheme as the original LDM model, while keeping c_θ and ϵ_θ unchanged.

To import initial designs from the structural gene database into the topology optimization process for representation and description, it is necessary to characterize structural genes using mathematical expressions. This article utilizes the VGG-19 model with pre-trained *ImageNet* weights to extract features of structural genes and compare them with features of optimization results.

The style feature differences between the structural gene described by $\boldsymbol{s}$ and the optimized structure described by $\boldsymbol{\rho}$ can be measured using the following loss function:

$$L(\boldsymbol{\rho}, \boldsymbol{s}) = L_{style}(\boldsymbol{\rho}, \boldsymbol{s}) + wL_{tv}(\boldsymbol{\rho}), \quad (3a)$$

where

$$L_{style}(\boldsymbol{\rho}, \boldsymbol{s}) = \sum_{l=1}^{L} w_{style}^l E_{style}, \quad (3b)$$

$$L_{tv}(\boldsymbol{\rho}) = \sum \left((\nabla_x \boldsymbol{\rho})^2 + \left(\nabla_y \boldsymbol{\rho}\right)^2\right)^{1.25}, \quad (3c)$$

with

$$E_{style}(\boldsymbol{\rho}, \boldsymbol{s}, l) = \frac{1}{4C^2 N_l^2 M_l^2} \sum_{m,n} (G_{mn}^l - A_{mn}^l)^2, \quad (3d)$$

$$G_{mn}^l(\boldsymbol{\rho}, l) = \sum_k R_{mk}^l R_{nk}^l, \quad (3e)$$

$$A_{mn}^{l}(\boldsymbol{s}, l) = \sum_{k} S_{mk}^{l} S_{nk}^{l}. \tag{3f}$$

In Equation (3), the L_{style} function computes the difference in feature map responses in terms of style between the structural gene and the current optimization structure; L_{tv} represents the total variation loss, which serves to enhance the spatial smoothness of the generated image, thus avoiding excessive pixelation in the results. The symbol w_{style}^{l} denotes the weight coefficients for each convolutional layer, while w represents the weight coefficient for the total variation loss, which can be manually selected based on the specific problem. The degree of influence of structural genes on the optimization structure can be controlled by adjusting the value of the $L(\boldsymbol{\rho}, \boldsymbol{s})$ function. R and S are the feature map responses of vectors $\boldsymbol{\rho}$ and $\boldsymbol{s}$ under the action of filtering functions. The symbol l indicates the number of layers in the network (total L); C represents the number of channels, which is 3 for RGB color images; S_{mk}^{l} and R_{mk}^{l} are the activations at position $k \in M_l$ by the m-th filter ($m \in N_l$)) at layer l; N_l is the number of filters at layer l; M_l is the size of the feature map; $\mathbf{G}^{l}$ and $\mathbf{A}^{l}$ are Gram matrices representing the inner product of the m-th and n-th feature maps at the l-th convolutional layer.

The content feature differences between the structural gene described by $\boldsymbol{s}$ and the optimized structure described by $\boldsymbol{\rho}$ can be measured using the following loss function:

$$L(\boldsymbol{\rho}, \boldsymbol{s}) = L_{sketch}(\boldsymbol{\rho}, \boldsymbol{s}) + wL_{tv}(\boldsymbol{\rho}), \tag{4a}$$

where

$$L_{sketch}(\boldsymbol{\rho}, \boldsymbol{s}) = \frac{1}{2} \sum_{m,k,l} \left(R_{mk}^{l} - S_{mk}^{l}\right)^{2}, \tag{4b}$$

Equation (5) presents the expression for text-driven topology optimization within the two-dimensional SIMP framework, with structural compliance as the objective function, considering volume constraints and the loss function $L(\boldsymbol{\rho}, \boldsymbol{s})$.

$$\begin{aligned} &\text{Find} \quad \boldsymbol{\rho}^{\mathsf{T}}, \boldsymbol{u} \\ &\text{Minimize} \quad I = \boldsymbol{f}^{\mathsf{T}} \boldsymbol{u} \\ &\text{S. t.} \\ &\mathbf{K}(\boldsymbol{\rho}) \boldsymbol{u} = \boldsymbol{f}, \\ &g_1(\boldsymbol{\rho}) = L(\boldsymbol{\rho}; \boldsymbol{s}) \leq \varepsilon, \\ &g_2 = \sum_{e=1}^{n} \rho_e \, v_e \leq \bar{V}, \\ &\boldsymbol{u} = \overline{\boldsymbol{u}}, \qquad \text{on } \Gamma_u, \\ &\rho_i \in \left[\underline{\rho}, 1\right] \; \forall \, i \in \Omega, \end{aligned} \tag{5}$$

where, n represents the total number of grids, and $\bar{V}$ is the upper limit of the available solid material volume. The structural gene is introduced in the form of the formal constraint function g_1.

3 Results

In this study, the material library results were obtained through fine-tuning based on two biological structures, as shown in Figure 2. Using the prompt "A black and white pattern of ammonites," a pattern similar to the features of ammonite sutures can be generated. Ammonite sutures are complex folded patterns on their shells that increase the contact area between the shell and the chamber septa, thereby enhancing the structural strength of the shell. This structure allowed ammonites to withstand deep-sea pressures and adapt to the deep-sea environment. For the Euplectella sp., its skeletal structure is composed of silica fibers, forming a highly ordered lattice structure. This structure provides great strength and stiffness while maintaining lightness and has the potential to prevent buckling deformation.

As illustrated in Figure 3a, the example considers a structure subjected to pressure from four sides. The result of the optimization design based on pure compliance minimization is displayed in Figure 3b, with a resulting compliance of $I = 186.089$. Incorporating the structural features of the Euplectella sp. into the topology optimization design, as shown in Figure 3d, results in a structure with a compliance of $I = 240.651$ (Figure 3c). Although some stiffness is sacrificed in this process, the physical properties of the Euplectella sp. are well preserved. In addition, the sponge structure extends axially, possessing the capability to resist compressive loads, while its performance in the tangential direction is not as significant. Under the condition of compression from four sides, the optimization results show characteristics similar to the microstructure of the cedar cross-section (Figure 3e). Cedars primarily bear wind loads, and their rectangular honeycomb structure is arranged in the transverse section to resist the bending caused by lateral wind loads. These two structures show commonalities in providing lightweight support and resistance to compressive deformation of the cell walls. From the analysis of this example, the structural adaptation trends in biological evolution can be observed.

4 Conclusions and Contributions

This study proposes an improved text-guided topology optimization design method based on deep learning techniques. To implement this method, a biomaterial database encompassing structural genes was constructed and integrated into topology optimization design. This integration introduces optimization strategies from nature, generating engineered structures that meet mechanical performance requirements and exhibit bio-inspired characteristics. Experimental validation demonstrates a novel paradigm of functional biomimetic design. Subsequent research will further explore the precise conjunction of structural design with natural optimization strategies.

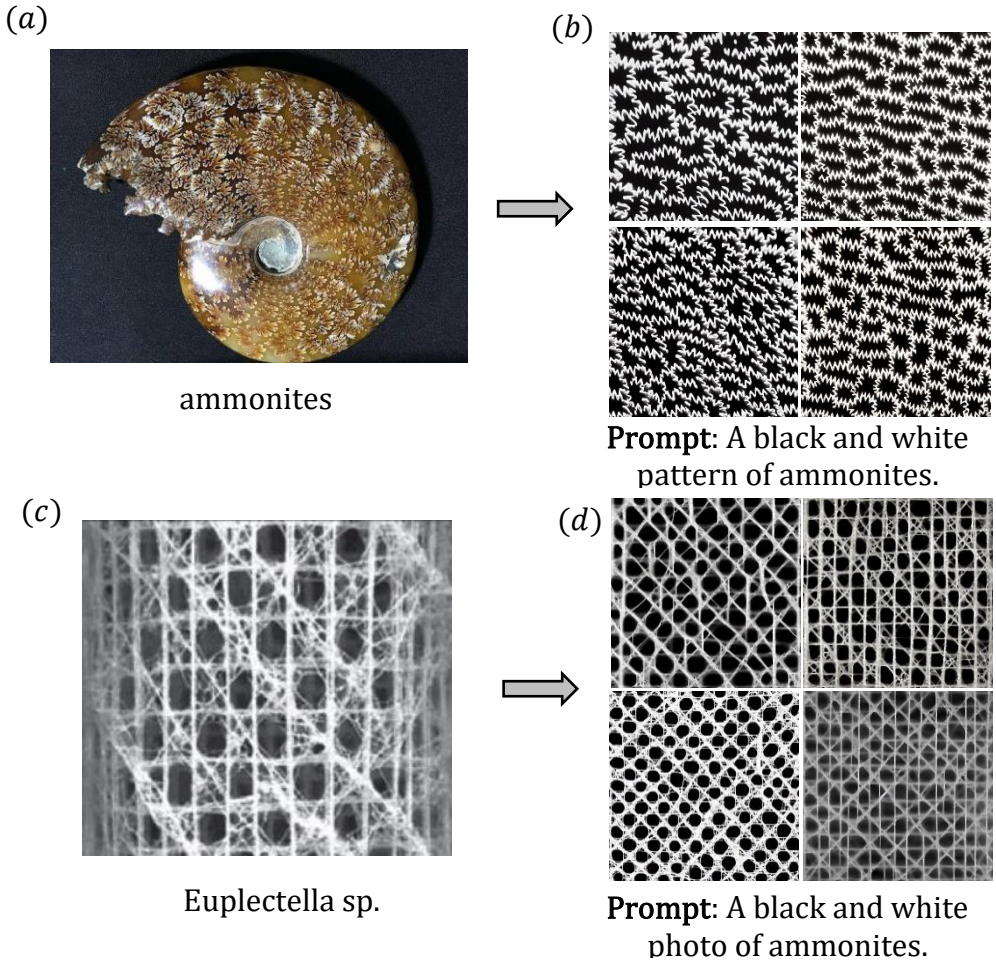

Figure 2: Text-guided material library fine-tuning results based on LDM.

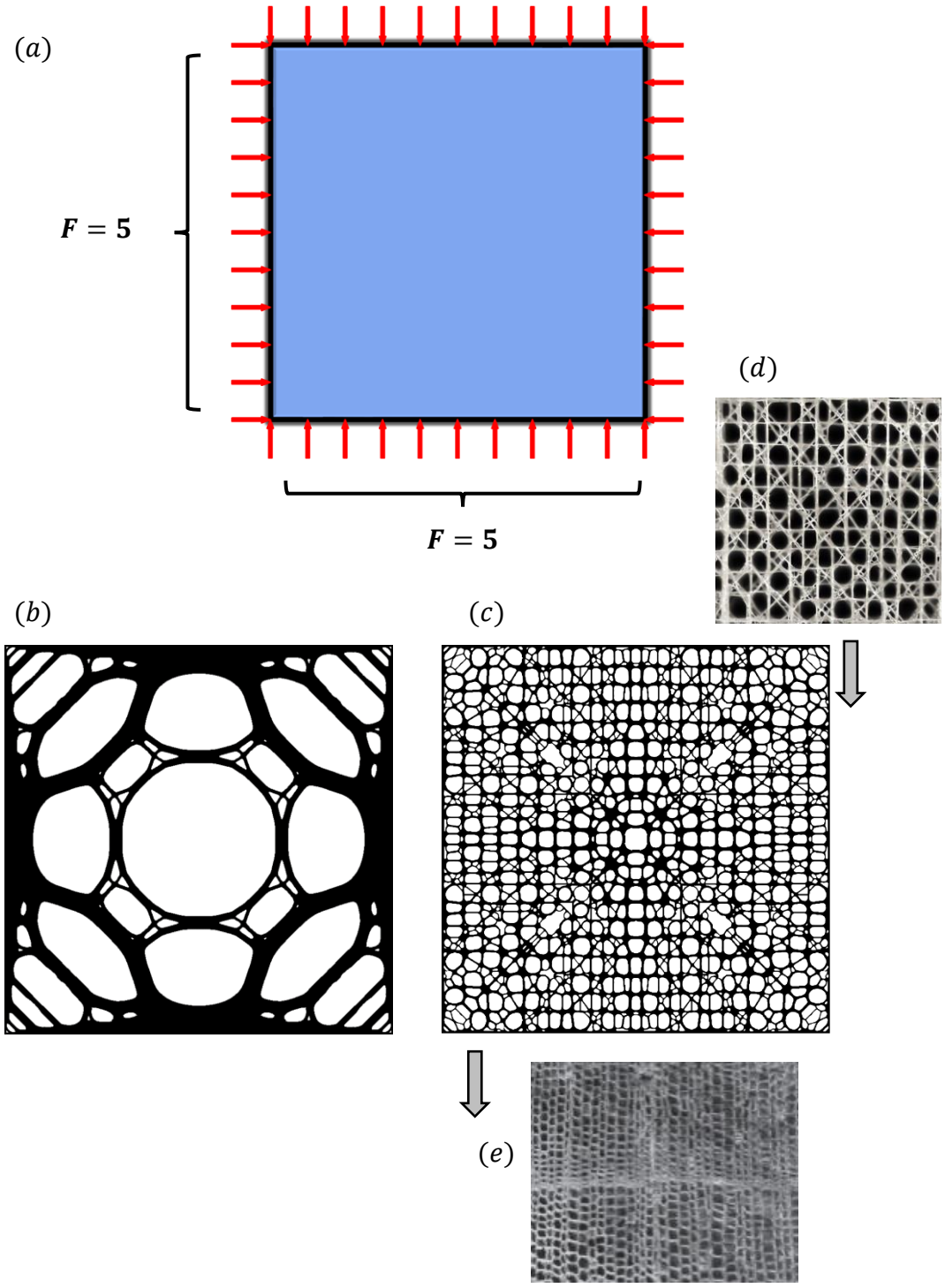

Figure 3: Topology optimization design example simulating biological evolution. (a) An example subjected to compression on four sides;(b) The pure compliance minimization result;(c) The optimized design referring to structural gene Euplectella sp.; (d) Structural gene Euplectella sp. obtained from Material library;(e) Microstructure of cedar wood.

References

[1] D. Nepal, S. Kang, K.M. Adstedt, et al, "Hierarchically structured bioinspired nanocomposites." Nature materials 22.1 (2023): 18-35.

[2] M.C. Fernandes, J. Aizenberg, J.C. Weaver, et al, "Mechanically robust lattices inspired by deep-sea glass sponges." Nature Materials 20.2 (2021): 237-241.

[3] H. Zheng, H. Mofatteh, M. Hablicsek, et al, "Dragonfly-Inspired Wing Design Enabled by Machine Learning and Maxwell's Reciprocal Diagrams." Advanced Science 10.18 (2023): 2207635.

[4] G.D. Bixler, B. Bhushan, "Fluid drag reduction with shark-skin riblet inspired microstructured surfaces." Advanced Functional Materials 23.36 (2013): 4507-4528.

[5] T. Yang, Z. Jia, H. Chen, et al, "Mechanical design of the highly porous cuttlebone: A bioceramic hard buoyancy tank for cuttlefish." Proceedings of the National Academy of Sciences 117.38 (2020): 23450-23459.

[6] Z. Shen, T.R. Neil, D. Robert, et al, "Biomechanics of a moth scale at ultrasonic frequencies." Proceedings of the National Academy of Sciences 115.48 (2018): 12200-12205.2

[7] R.O. Prum, T. Quinn, R.H. Torres, "Anatomically diverse butterfly scales all produce structural colours by coherent scattering." Journal of Experimental Biology 209.4 (2006): 748-765.4

[8] B.D. Wilts, B. Apeleo Zubiri, M.A. Klatt, et al, "Butterfly gyroid nanostructures as a time-frozen glimpse of intracellular membrane development." Science advances 3.4 (2017): e1603119.

[9] R. Rombach, A. Blattmann, D. Lorenz, et al, "High-resolution image synthesis with latent diffusion models." Proceedings of the IEEE/CVF conference on computer vision and pattern recognition. 2022.

[10] C. Schuhmann, R. Vencu, R. Beaumont, et al, "Laion-400m: Open dataset of clip-filtered 400 million image-text pairs." arXiv preprint arXiv:2111.02114 (2021).

[11] J. Devlin, M.W. Chang, K. Lee, et al, "Bert: Pre-training of deep bidirectional transformers for language understanding." arXiv preprint arXiv:1810.04805 (2018).

[12] R. Gal, Y. Alaluf, Y. Atzmon, et al, "An image is worth one word: Personalizing text-to-image generation using textual inversion." arXiv preprint arXiv:2208.01618 (2022).